Wind Energy Applications of Unified and Dynamic Turbulence Models

Stefan Heinz and Harish Gopalan

Abstract This study investigates linear and nonlinear dynamic LES and unified RANS-LES models obtained by stochastic analysis regarding the simulation of the atmospheric boundary layer. The advantages of dynamic LES methods are their accuracy, the ability to account for anisotropy and backscatter, and their computational stability. The advantage of unified RANS-LES models is their ability to provide results like LES for a fraction of the cost of LES. Two applications are considered: (i) turbulent boundary layer simulations on fine grids, which were performed to demonstrate the suitability of models for turbulent boundary-layer turbulence studies, and (ii) neutral boundary layer simulations on coarse grids, where subgrid models have to contribute significantly. On fine grids, all models perform comparably. On coarse grids, a nonlinear dynamic model provides the most accurate results. A nonlinear unified RANS-LES model is shown to be well applicable as a low cost alternative.

1 Introduction

There is a growing interest in using wind energy to provide electricity all around the globe. For example, a recent report by the Department of Energy suggests the possibility of providing 20% of the electricity in the U.S. by wind energy in 2030. A significant problem of existing wind farms is their relatively low efficieny. Due to the wind turbine wakes, the efficiency of wind farms is reduced by 20 to 50 percent compared to turbines in isolation [1]. Therefore, there is a significant need for research related to the interaction of wind turbines with the surrounding air flow.

Stefan Heinz
Department of Mathematics, University of Wyoming, 1000 E. University Avenue, Laramie, WY 82071, USA e-mail: heinz@uwyo.edu

Harish Gopalan
Department of Mechanical Engineering, University of Wyoming, 1000 E. University Avenue, Laramie, WY 82071, USA e-mail: hgopalan@uwyo.edu

The only way to obtain a comprehensive understanding of wind farm processes is the use of numerical simulations. However, such simulations face significant problems related to the consistency of equations, the generality of equations, and the computational cost of simulations. A very promising approach to find general solutions for these questions is the development of turbulence models on the basis of stochastic analysis. Unified combinations of Reynolds-averaged Navier-Stokes (RANS) equations with large eddy simulation (LES) equations, and dynamic LES equations were presented recently by Heinz [2, 3]. The advantages of dynamic LES methods are their accuracy, the ability to account for anisotropy and backscatter, and their computational stability. The advantage of unified RANS-LES models is their ability to provide results like LES for a fraction of the cost of LES. Details about the characteristic features of these methods and applications to channel flow simulations can be found elsewhere [4–6].

The purpose of this paper is to report applications of these unified and dynamic methods to turbulent boundary-layer turbulence studies relevant to wind energy applications. The turbulence models applied will be described in Sect. 2. Section 3 deals with a presentation of the numerical methods applied and problems considered. The results obtained by means of unified and dynamic LES models are discussed in Sect. 4. Section 5 summarizes the conclusions of these studies.

2 Unified and Dynamic Model Equations

For the incompressible flow considered, the LES equations for filtered velocities $\widetilde{U}_i$, where $i = 1,2,3$, are given by the incompressibility constraint $\partial \widetilde{U}_i/\partial x_i = 0$ and the momentum equation

$$\frac{\widetilde{D}\widetilde{U}_i}{\widetilde{D}t} = -\frac{1}{\rho}\frac{\partial \widetilde{p}}{\partial x_i} + 2\nu\frac{\partial \widetilde{S}_{ik}}{\partial x_k} - \frac{\partial \tau_{ik}}{\partial x_k}. \tag{1}$$

Here, $\widetilde{D}/\widetilde{D}t = \partial/\partial t + \widetilde{U}_k\partial/\partial x_k$ denotes the filtered Lagrangian time derivative, $\widetilde{p}$ is the filtered pressure, ρ is the constant fluid mass density, ν is the constant kinematic viscosity, τ_{ij} is the subgrid-scale (SGS) stress tensor, and $\widetilde{S}_{ij} = (\partial\widetilde{U}_i/\partial x_j + \partial\widetilde{U}_j/\partial x_i)/2$ is the rate-of-strain tensor. The sum convention is used throughout this paper. The SGS stress is given by the quadratic model [2, 3]

$$\tau_{ij} = \frac{2}{3}k\delta_{ij} - 2\nu_t\widetilde{S}_{ij} - 3\frac{\nu_t^2}{k}\left[\widetilde{S}_{ik}\widetilde{\Omega}_{kj} + \widetilde{S}_{jk}\widetilde{\Omega}_{ki} - 2\widetilde{S}_{ik}\widetilde{S}_{kj} + \frac{2}{3}\widetilde{S}_{nk}\widetilde{S}_{kn}\delta_{ij}\right]. \tag{2}$$

Here, $k = \tau_{nn}/2$ refers to the SGS kinetic energy and $\widetilde{\Omega}_{ij} = (\partial\widetilde{U}_i/\partial x_j - \partial\widetilde{U}_j/\partial x_i)/2$ is the rate-of-rotation tensor. The SGS viscosity is given by $\nu_t = C_k L_m\sqrt{k}$, where C_k is a constant. The choice of the model length scale L_m decides about the model applied. This length scale is $L_m = \Delta$ if the dynamic model is used, and $L_m = \min(\Delta, L)$ if the unified model is applied, respectively. Here, L is defined by $L = k^{1.5}/\varepsilon$, and Δ

is the filter width. The SGS kinetic energy and dissipation rate ε are calculated by

$$\frac{\widetilde{D}k}{\widetilde{D}t} = \frac{\partial}{\partial x_k}\left[(\nu + \nu_t)\frac{\partial k}{\partial x_k}\right] - \tau_{ij}\frac{\partial \widetilde{U}_j}{\partial x_i} - \frac{k^{3/2}}{L_m}, \tag{3}$$

$$\frac{\widetilde{D}\varepsilon}{\widetilde{D}t} = -C_1\frac{\varepsilon}{k}\tau_{ij}\frac{\partial \widetilde{U}_j}{\partial x_i} - C_2\frac{\varepsilon^2}{k} + \frac{\partial}{\partial x_k}\left[(\nu + \nu_t/\sigma_e)\frac{\partial k}{\partial x_k}\right]. \tag{4}$$

Here, $C_1 = 1.21$, $C_2 = 1.92$ and $\sigma_e = 1.3$ are usually applied constants.

The unified and dynamic models calculate the constants in different ways. Unified models apply $C_k = 1/9$. A linear unified model (LUM) neglects the quadratic term in Eq. (2), whereas a nonlinear unified model (NUM) applies Eq. (2). A linear dynamic model (LDM) neglects the quadratic term in Eq. (2) and calculates C_k dynamically. A nonlinear dynamic model (NDM) applies Eq. (2) and calculates the C_k values of linear and nonlinear terms separately by a dynamic method [3]. More details about these unified and dynamic methods can be found elsewhere [2–6].

3 Numerical Method and Problems Considered

Simulations were performed by using a finite-volume based method inside the OpenFOAM CFD Toolbox. The convection term in the momentum equation was discretized using a second-order central difference scheme. The PISO algorithm was used for the pressure-velocity coupling. The resulting algebraic equation for all the flow variables except pressure has been solved iteratively using a preconditioned bi conjugate gradient method with a diagonally incomplete LU preconditioning at each time step. The Poisson equation for the pressure was solved using an algebraic multi-grid (AMG) solver. When the scaled residual became less than 10^{-6}, the algebraic equation was considered to be converged. Time marching was performed using a second-order backward difference scheme. The time step was modified dynamically to ensure a constant CFL number of 0.5. Periodic boundary conditions have been employed along the streamwise and spanwise directions for all the flow variables. The wall-function approach was used to implement the boundary condition at the bottom of the domain while a stress free boundary condition was applied at the domain top. The consequence of using the wall-function approach is the need to replace negative values of the effective diffusivity in k and ε equations by zero if the dynamic approach is used.

Table 1 Set-up of the numerical simulations.

Parameters	Wind tunnel	Neutral boundary layer
Domain	4.32 m $*$ 0.72 m $*$ 0.46 m	4 km $*$ 2 km $*$ 1.5 km
Grid	$350 * 80 * 80$	100 * 100 * 40
Roughness length (z_o)	0.03 mm	0.1 m

Two problems were considered, see the domain, grid resolution, and other parameters provided in Table 1. Regarding the wind tunnel simulations, the imposed pressure gradient drives the flow, whereas the geostrophic wind is used to drive the neutral boundary layer simulations. The motivation for performing wind tunnel simulations on fine grids is to show the suitability of models for atmospheric boundary layer (ABL) turbulence studies. But ABL LES is almost always performed on coarse grids. This motivates the application of turbulence models to neutral ABL simulations according to the benchmark problem of Andren et al. [7]. It should be noted that the grid resolution applied here is finer than the grids used in previous studies because a second-order central difference scheme is used here in the streamwise and spanwise directions, whereas spectral methods were used in previous studies. Systematic grid dependency studies are planned to analyze the performance of unified RANS-LES models in comparison with dynamic methods on coarse grids. We did not perform boundary condition sensitivity tests. Sullivan et. al [8] showed that lower boundary conditions using different wall-functions provide similar results.

4 Results and Discussion

The fine-grid comparisons of the mean streamwise velocity and Reynolds normal stress obtained from the dynamic and unified models considered with experimental data [9] are shown in Fig. 1. Results obtained by using the Lagrangian averaged scale dependent dynamic model (LASDD) [10] are also shown. The results obtained with the different models show a good agreement with each other and the experimental data. The NDM optimally predicts the peak of the Reynolds normal stress.

The coarse-grid comparisons of the normal components of the stress τ_{ij} obtained from the two unified and two dynamic models considered are shown in Fig. 2. For coarse grids, the SGS stress has to provide a main contribution to the total stress, which is known to be highly anisotropic. Hence, the SGS stress has to reflect this anisotropy. However, Fig. 2 shows that not all the models considered provide this anisotropy. The linear LUM and LDM predict isotropic stresses because they do not involve nonlinear terms. The nonlinear NUM and NDM predict an anisotropy of stresses. The anisotropy provided by the NUM is very small, whereas the prediction of the NDM shows characteristic features observed, e.g., for channel flow.

Another relevant difference between the nonlinear NUM and NDM can be seen in Fig. 3, which shows the vertical profiles of the normalized modeled, resolved, and total Reynolds shear stress. In LES, the resolved stress should continuously increase with the vertical height in correspondence to the behavior of the total stress. The NUM is not capable of simulating this shear stress behavior: the resolved stress has a discontinuity, and it is smaller than the modeled stress close to the surface. On the other hand, the NDM correctly describes this shear stress behavior: the resolved stress increases linearly with the height. The reason for the ability of the NDM to correctly describe the shear stress behavior is the inclusion of backscatter which tranfers kinetic energy from the modeled to the resolved scales [8].

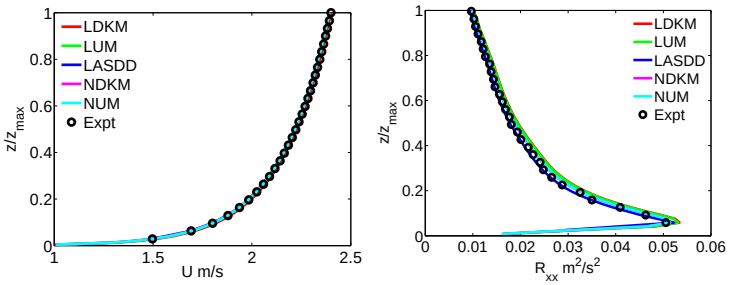

Fig. 1 Comparison of unified and dynamic models and the LASDD model with wind tunnel experiments [9]: (a) mean streamwise velocity, (b) streamwise Reynolds normal stress.

5 Conclusions

The NDM model is found to be the most accurate model due to its ability to account for anisotropy and backscatter. Pictures of instantaneous streamwise velocities, which are not presented here, do also show that the NDM is capable of excellently representing the small-scale structure of turbulence. The NUM represents a valid alternative if computationally more efficient simulations have to be performed.

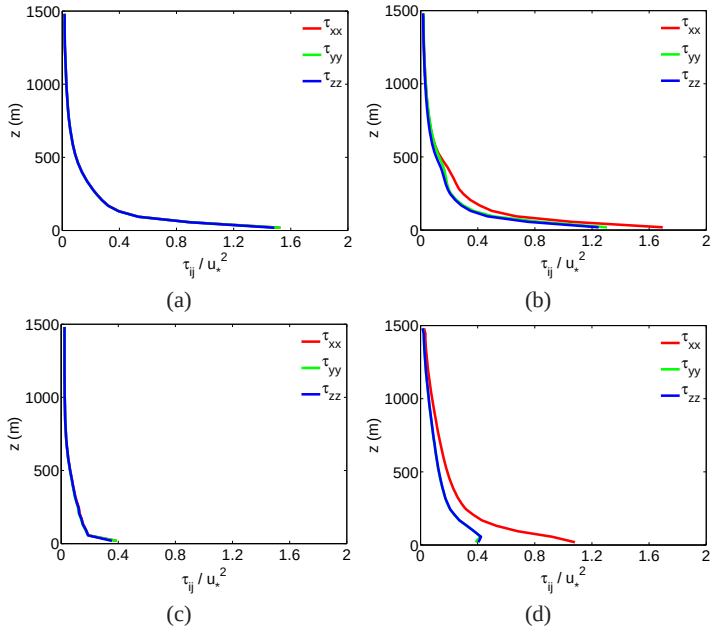

Fig. 2 Comparison of normalized modeled normal stresses obtained for the neutral ABL: (a) LUM, (b) NUM, (c) LDM, and (d) NDM. Here, u_* is the friction velocity and z is the vertical height.

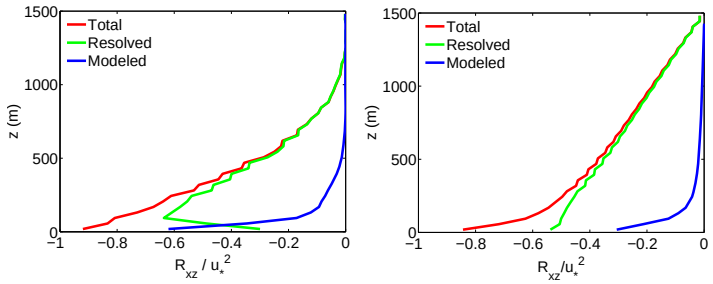

Fig. 3 Comparison of the normalized modeled, resolved, and total Reynolds shear stress: (a) NUM and (b) NDM. Here, u_* is the friction velocity and z is the vertical height.

References

[1] J. O. Dabiri. Potential order-of-magnitude enhancement of wind farm power density via counter-rotating vertical-axis wind turbine arrays. *IRESR*, 3(4): 043104/1–12, 2011.

[2] S. Heinz. Unified turbulence models for LES and RANS, FDF and PDF simulations. *Theor. Comp. Fluid Dyn.*, 21(2):99–118, 2007.

[3] S. Heinz. Realizability of dynamic subgrid-scale stress models via stochastic analysis. *Monte Carlo Methods Appl.*, 14(4):311–329, 2008.

[4] S. Heinz, H. Gopalan, and M. Stöllinger. A unified RANS-LES model. Part 1. Computational model development. *J. Comput. Phys.*, 2012.

[5] H. Gopalan, S. Heinz, and M. Stöllinger. A unified RANS-LES model. Part 2. Model accuracy and computational cost. *J. Comput. Phys.*, 2012.

[6] S. Heinz and H. Gopalan. Realizable versus non-realizable dynamic subgrid-scale stress models. *Phys. Fluids*, 24:submitted, 2012.

[7] A. Andren, A. R. Brown, P. J. Mason, J. Graf, U. Schumann, C. H. Moeng, and F. T. M. Nieuwstadt. Large-eddy simulation of a neutrally stratified boundary layer: A comparison of four computer codes. *Q. J. Roy. Meteo. Soc.*, 120(520): 1457–1484, 1994.

[8] P. P. Sullivan, J. C. McWilliams, and C. H. Moeng. A subgrid-scale model for large-eddy simulation of planetary boundary-layer flows. *Bound-Lay. Meteorol.*, 71(3):247–276, 1994.

[9] L. P. Chamorro and F. Porté-Agel. A wind-tunnel investigation of wind-turbine wakes: boundary-layer turbulence effects. *Bound-Lay. Meteorol.*, 132(1):129–149, 2009.

[10] Y. T. Wu and F. Porté-Agel. Large-eddy simulation of wind-turbine wakes: evaluation of turbine parametrisations. *Bound-Lay. Meteorol.*, 138(3):345–366, 2011.